Chapter 3
A Look at Overfitting in Source Estimation Problems

Steven Carter

Abstract Inverse source estimation (ISE) is a fundamental technique that is widely studied in transfer path analysis (TPA) and multiple-input/multiple-output (MIMO) vibration testing. It is commonly accepted that errors in the frequency response functions (FRFs) and target responses can lead to overfitting errors, which can present as over-predictions of the source amplitudes. These overfitting errors are generally attributed to the ISE problem being ”ill-posed”, but there seems to be limited discussion in the literature about how specific errors (such as modeling errors) lead to overfitting. This work describes a study that was done to gain a deeper understanding of the causes of overfitting by evaluating how the FRF and response errors impact the ISE problem differently. It will evaluate how common techniques that are used to evaluate and mitigate overfitting (such as cross-validation and regularization) are influenced by the different types of error and will share the lessons that were learned over the course of the study.

Keywords TPA · MIMO Testing · Force Reconstruction

Introduction

Inverse source estimation (ISE) is a fundamental technique in noise and vibration engineering that is widely studied in force reconstruction [1], transfer path analysis (TPA) [2], and multiple-input/multiple-output (MIMO) vibration testing [3]. The most common ISE technique uses the frequency response function (FRF) equation of motion, as shown in (1) where $\{X\}$ is a vector of response linear spectra, $[H]$ is a matrix of FRFs, and $\{F\}$ is a vector of source linear spectra (forces for force reconstruction and TPA, shaker drives for MIMO vibration testing).

$$\{X\} = [H]\{F\} \tag{1}$$

The sources are recovered from a set of target responses and FRFs with (2) where $[\bullet]^{\dagger}$ indicates the pseudo-inverse of the FRF matrix.

$$\{F\} = [H]^{\dagger}\{X\} \tag{2}$$

While force reconstruction and TPA commonly utilize the linear spectra formulation, MIMO vibration testing typically uses the cross-power spectral density (CPSD) formulation that is shown in (3) and (4). In these equations $[G_{xx}]$ is a (square) matrix of response CPSDs, $[G_{ff}]$ is a (square) matrix of source CPSDs, and $[\bullet]^{*}$ indicates the conjugate transpose of the given matrix.

$$[G_{xx}] = \{X\}\{X\}^{*} = \{[H]\{X\}\}\{[H]\{X\}\}^{*} = [H][G_{ff}][H]^{*} \tag{3}$$

$$[G_{ff}] = [H]^{\dagger}[G_{xx}][H]^{\dagger^{*}} \tag{4}$$

Source estimation by FRF matrix inversion is an ill-posed process, which can lead to overfitting errors [4, 5], resulting in erroneously high source amplitudes since the inverse problem is fitting errors in the FRFs or responses. There has been significant research into methods that can be used to mitigate the overfitting errors, either through regularization [6–9], transformations [10–12], or thoughtful selection of response degrees of freedom (DOFs) [13, 14]. These methods have been shown to dramatically reduce overfitting, but there has been little discussion (in the ISE literature) on the root causes for the overfitting errors and why the mitigation techniques work. As such, a study was performed to better understand overfitting. This paper details the results of that study, which attempted to address the following questions:

Steven Carter
Sandia National Laboratories, P.O. Box 5800 – MS0557, Albuquerque, NM, 87185
e-mail: spcarte@sandia.gov

Walter D’Ambrogio, et al. (eds.), *Dynamic Substructuring & Transfer Path Analysis, Vol. 4*, Conference Proceedings of the Society for Experimental Mechanics Series, https://doi.org/10.13052/97887-438-0149-8_3

- What is the theoretical mechanism for the overfitting error in ISE problems?
- How do the different sources of ISE error (i.e., modeling errors or measurement noise in the target responses) align with the theoretical mechanism for overfitting?
- Does cross-validation work as a method for identifying an overfit solution? This question is being asked since previous experience [4] has shown that cross-validation may be insufficient for identifying overfitting.
- How does regularization improve the source estimation, based on the theoretical mechanism for overfitting?

The remainder of this paper is structured as follows. First, a theoretical model for overfitting will be introduced. Second, the theoretical model for overfitting will be applied to cross-validation and regularization to gain a deeper understanding of the methods. Third, various test cases will be performed on a numerical model to evaluate hypotheses related to the theory of overfitting, how regularization works to mitigate overfitting, and when cross-validation works to identify overfitting. Lastly, there will be conclusions on the results of the study.

Theoretical Model for Overfitting in Source Estimation

The fundamental sources of error (excluding model form error) in an ISE problem should be determined before a theoretical model for overfitting can be developed. In this work, it is assumed that the potential errors can be modeled as additive errors to the FRFs or target responses, as shown in (5) and (6), where ε is an error term for the quantity that is described in the superscript. Note that the error term for the FRFs will be referred to as "modeling errors" and the error term for the target responses will be referred to as "response errors" for the remainder of this paper. Also note that these errors could be applied to either the linear or power spectra version of the ISE equations but are only being shown for linear spectra to simplify the algebra.

$$\{X\} = \left[[H] + \left[\varepsilon^{FRF}\right]\right]\{F\} \tag{5}$$

$$\{\{X\} + \{\varepsilon^{response}\}\} = [H]\{F\} \tag{6}$$

One can start to develop an intuitive understanding of the overfitting error if (5) and (6) are solved to estimate the sources, as shown in (7) and (8).

$$\{F\} = \left[[H] + \left[\varepsilon^{FRF}\right]\right]^{\dagger}\{X\} \tag{7}$$

$$\{F\} = [H]^{\dagger}\{\{X\} + \{\varepsilon^{response}\}\} = [H]^{\dagger}\{X\} + [H]^{\dagger}\{\varepsilon^{response}\} \tag{8}$$

A high-level reason for overfitting is easily seen in (8) since the response error term turns into an additive error in the sources. Similar logic for overfitting can be applied when there are modeling errors, as shown in (7). However, the additive error in the FRFs does not become an additive error in the sources since the pseudo-inverse inseparably combines the FRFs with the modeling errors. Further engineering intuition can be developed on overfitting when the inverse problem is viewed through the singular components of the FRF matrix, as shown in (9) and (10) where $[U]$ is a rectangular matrix of left singular vectors, $[S]$ is a diagonal matrix of singular values, and $[V]$ is a square matrix of right singular vectors.

$$[H] = [U][S][V]^{*} \tag{9}$$

$$\{F\} = [V][S]^{\dagger}[U]^{*}\{X\} \tag{10}$$

The first two matrix operations (from the right) in (10), which are isolated in (11), can be viewed as a response transformation [15] that has been scaled by the inverse of the singular values. Response transformations have been widely studied in structural dynamics and there are several theoretical formulations depending on the use case. Examples for the different types of response transformations include the virtual point transformation (VPT) in TPA and substructuring [10, 16, 17], output transformations in MIMO vibration testing [18], and modal filtering [19].

$$\{F\} = [V]\left\{X^{Transformed}\right\} \rightarrow \left\{X^{Transformed}\right\} = [S]^{\dagger}[U]^{*}\{X\} \tag{11}$$

The modal filtering perspective on the transformation seems to be the most appropriate for this case since the left singular vectors of the FRF matrix are combinations of the mode shapes of the system [20]. Consequently, the transformation can be described similarly to a modal filtering operation. In this case, the physical responses are transformed into "singular responses" through a least squares projection onto the left singular vectors of the FRF matrix. The term singular response is being used to describe the transformed response, instead of the term "modal responses" (which is used in modal filtering), because the transformation basis is singular vectors instead of mode shapes.

Recent work in modal filtering [21] has highlighted two main errors that could occur in the transformation when there are response or modeling errors in the ISE problem, which could lead to mismatches between the left singular vectors of the FRF matrix and the deflection shapes in the target responses:

1. It may be impossible for the left singular vectors of the FRF matrix to be combined in a way to fit the deflection shapes in the target responses, eliminating some information from the inverse problem. For example, a test set-up will never be able to excite a particular mode of a system if the excitation locations are at a nodal line of that mode.
2. Alternatively, it may be possible for the left singular vectors of the FRF matrix to be combined in a way to fit the deflection shapes in the target response, even if it is inappropriate to do so. For an example, a complicated set of singular vectors may be able to fit random measurement noise in the target responses even though the measurement noise represents a "non-physical" response that does not match the structural dynamics of the structure.

It is hypothesized that the second transformation error that was described above is the root cause for overfitting in ISE problems because spurious combinations of singular vectors fit the target responses in an erroneous manner, causing the singular responses to have excessive amplitudes. The singular response errors in-turn will cause excessively high source amplitudes. It is important to note that the condition number FRF matrix should also be considered in overfitting, since the amplitude of the sources is directly related to the amplitude of the inverted singular values, as shown in (11). However, the author argues that the root cause for overfitting is the same, regardless of if the overfitting is significant to the ISE problem.

Cross Validation as a Method to Identify Overfitting

Cross validation (CV) is typically used in ISE to test if a set of sources can recreate the "true" response at all locations on a structure, not just the locations that were used to compute the sources. The typical process for CV in ISE (based on the authors experience) is to split the full set of target response DOFs into a "training set" and "validation set". The training set is used to compute the sources while the validation set is used to assess the predictive capability of the sources. This assessment is done by computing the responses at the validation DOFs with the sources that were estimated with the training dataset. The recomputed and target responses at the validation DOFs are then compared to each another to assess the predictive capability of the estimated sources, which is rated depending on how well the responses match.

The basic process for CV is relatively straight-forward and seems to provide a reasonable check for overfitting at first glance. However, there is an important requirement that the training and validation datasets be independent from one another [22]. From a modal perspective, this requirement means that the training and validation DOF sets should describe unique portions of the deflection shapes.

Essentially, the CV check (as described above) is checking to see if the estimated sources can reconstruct the deflection shapes that are described by both the training and validation DOFs sets. Note that this check is different than validating that the estimated sources can reconstruct the correct deflection shape all over the structure, for two reasons. First, significant portions of the overall deflection shapes of the structure may be neglected, if the training and validation DOF sets are poorly chosen (e.g., a critical component is left out). Second, the validation DOF set may not describe a unique portion of the deflection shapes of the structure, compared to the training DOF set, meaning that the CV check would not provide new information. Consequently, it is hypothesized that the CV check may not be sensitive to overfitting unless the training and validation DOFs are carefully chosen. Further, it is hypothesized that it may be difficult to obtain a meaningful CV check in cases where there are several target response DOFs that provide a good description of the deflection shapes of the structure.

It is important to note that the above hypothesis about CV should *not* be interpreted to say that CV checks are not useful. Rather, it is pointing to the fact that practitioners should carefully design validation experiments, so they are significant for the problem at-hand. For example, a CV check could be used in a way to validates that the sources are sufficient to recreate the responses at any point, on one version of a structure (i.e., the goal in a MIMO test). However, this same CV check may not be able to validate the sources are generic to any version of a structure (i.e., the goal in component based TPA), meaning that a different type of check (that spans multiple versions of the structure) should be used.

Regularization as a Method to Mitigate overfitting

Regularization is commonly used to mitigate overfitting in ISE problems [6-9]. The most common regularization methods for ISE are the truncated singular value decomposition (TSVD) and Tikhonov regularization. The equations for these methods are shown in (12) and (13), where N is a tunable parameter for the number of singular values to retain in the TSVD (the remaining values are set to zero) and λ is a tunable regularization parameter for Tikhonov regularization.

$$\{F\} = [V]\,[S\,(1:N)]^{\dagger}[U]^{*}\,\{X\} \tag{12}$$

$$\{F\} = [V]\,\frac{[S]}{[S]^{*}\,[S]+\lambda}[U]^{*}\,\{X\} \tag{13}$$

It is useful to partition the regularized ISE equations in the same manner as (11), as shown in (14) and (15) for the TSVD and Tikhonov regularization, respectively.

$$\{F\} = [V]\left\{X^{Transformed}\right\} \rightarrow \left\{X^{Transformed}\right\} = [S\,(1:N)]^{\dagger}[U]^{*}\,\{X\} \tag{14}$$

$$\{F\} = [V]\left\{X^{Transformed}\right\} \rightarrow \left\{X^{Transformed}\right\} = \frac{[S]}{[S]^{*}\,[S]+\lambda}[U]^{*}\,\{X\} \tag{15}$$

Both (14) and (15) show that both the TSVD and Tikhonov regularization tend to reduce the amplitude of the estimated sources, which is an effect that is known as shrinkage in the statistical literature [22]. The TSVD reduces the amplitudes of the estimated sources by eliminating the small singular values of the FRF matrix, which would become large when inverted. Tikhonov regularization works similarly to the TSVD, but it increases the amplitude of the small singular values (reducing their inverted value), rather than eliminating them (and the associated singular vectors) from the inverse problem.

Comparing the effect of the TSVD and Tikhonov regularization to the hypothesis for overfitting, it is evident that both methods assume that the small singular values (and associated singular vectors) are the primary cause of overfitting. Put more plainly, both methods assume that the significant left singular vectors (associated with the large singular values) in the FRFs are a good match to the primary deflection shapes in the target responses. However, there may be mismatches between the minor deflection shapes in the FRFs and target responses, which are associated with the small singular values of the FRF matrix. As previously described, the mismatches could lead to spurious singular responses, so the singular responses that are associated with the small singular values should be eliminated or made less significant to the ISE problem, which is how the TSVD and Tikhonov regularization mitigate overfitting.

Other forms of regularization, such as the least absolute shrinkage and selection operator (LASSO) and the elastic net [9, 23, 24], also exist for ISE problems. These methods perform both a shrinkage function (similar to the TSVD and Tikhonov regularization) and a subset selection function [22, 25], where source DOFs may be automatically set to zero if they are considered mathematically insignificant to the ISE problem. These methods are mentioned here for completeness but are considered outside of the scope of this work since they are not commonly used ISE and are significantly more mathematically complex than the TSVD and Tikhonov regularization.

Example Problem for the Overfitting Study

The previously mentioned hypotheses were tested on numerical models of the round robin system for the substructuring technical division of the Society of Experimental Mechanics [26, 27]. An image of the reduced modal model of the system is shown in Figure 1. Two versions of the model were used in this study, a calibrated finite element model of the system and an experimental modal model of the system, where the experimental modal model was used for the finite element (FE) model calibration. Both of these models were developed in the work described in [5]. These models were used for the overfitting study because they are reasonably similar, allowing for a version of the model that represents the truth and a version of the model with minor modeling errors. Note that the FE model was used as the truth model in this case, since it could allow for more in-depth analysis than the experimental modal model, if necessary. The FE model will be referred to as the "truth model" and the experimental modal model will be referred to as the "test model" for the rest of this paper.

The differences between the truth and test models are shown via a modal assurance criterion (MAC) comparison (for the elastic modes) in Figure 2 and a frequency difference comparison between high MAC modes (MAC values greater than 0.9) is shown in Figure 3. The truth and test shapes generally have high MAC values, with a single match for most mode except for mode three in the truth model, which matches two test modes. Lower MAC values are more common at higher frequencies, with the lowest MAC value being $\sim$0.38. The frequency difference comparison shows that the high MAC modes (with a MAC value greater than 0.9) have a good frequency match, with the highest difference being $\sim$3%. Note that the modal damping ratio for all modes in both the truth and test models was set to 0.005, which is why only the shapes and frequencies were compared to show the similarities and differences in the models.

Three sets of triaxial response DOFs were selected on the wing to use as the target responses in the overfitting study. The reason for having three sets of response DOFs was to have two DOF sets that could be used as training sets in the ISE and one

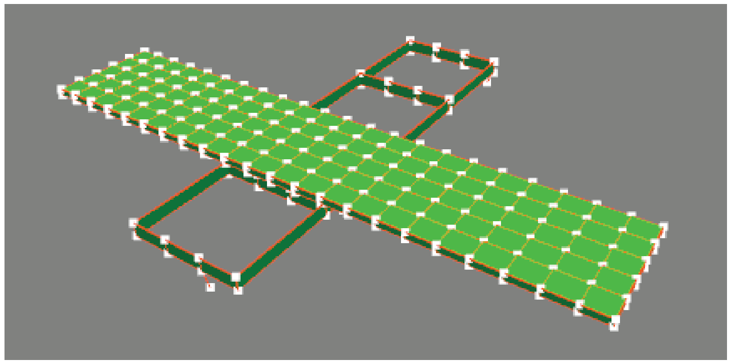

Fig. 1 The reduced modal model of the round robin system that was used to test the hypotheses in the overfitting study.

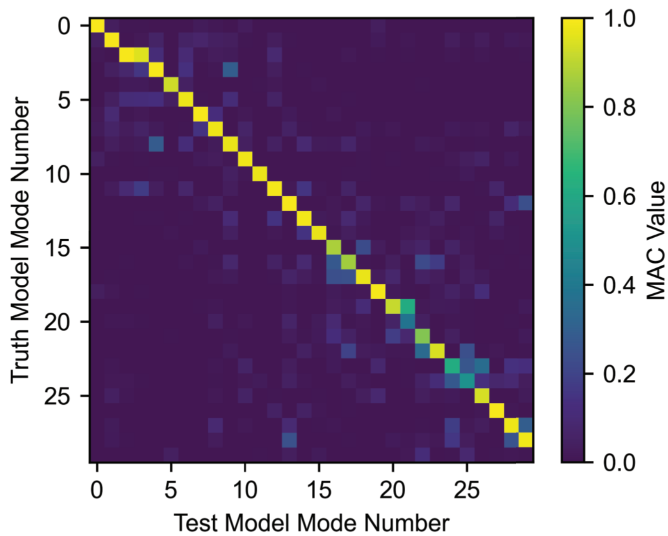

Fig. 2 MAC comparison between the modes in the truth and test models for the overfitting study.

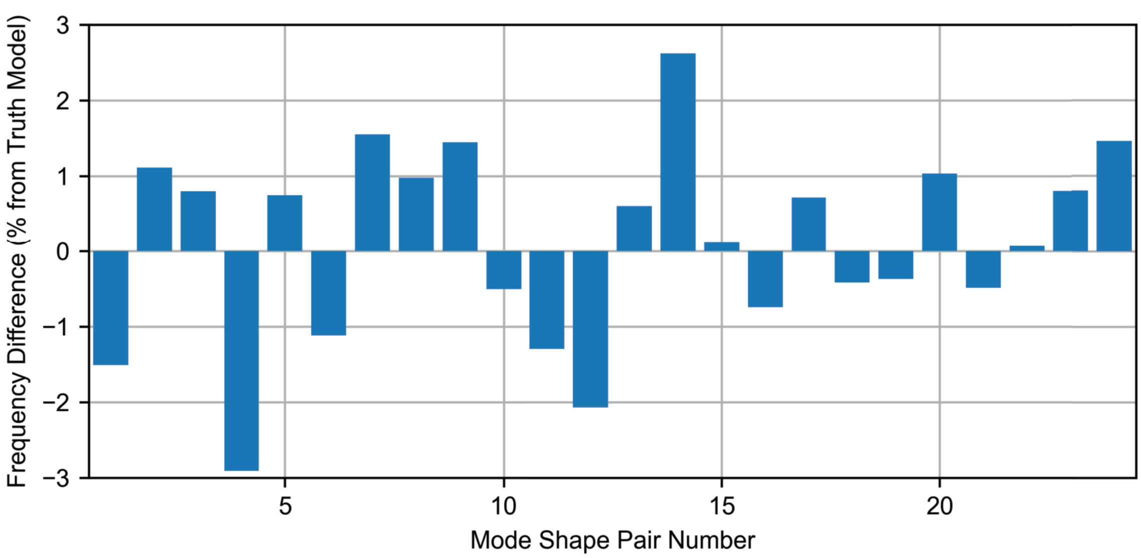

Fig. 3 Frequency difference comparison between high MAC modes in the truth and test models for the overfitting study.

validation DOF set that could be used for a CV check. One training set contained “good” response DOFs that describe the response deflection shapes well, and the other training set contained “bad” response DOFs that poorly describe the response deflection shapes. Consequently, it is assumed that the validation DOF set will *not* add independent information to the ISE problem when the good DOFs are used in the training set (since the deflection shapes are well defined by the good DOFs) but will add independent information when the bad DOFs are used in the training set (since the bad DOFs poorly describe the deflection shapes). As a result, the different DOF sets make it possible to test the previously described hypothesis on CV checks, depending on if the validation DOFs can identify overfitting when the sources are estimated with responses at the good and bad DOFs (where comparisons between the estimated and truth sources are the ultimate check).

The DOF sets were objectively selected with an effective independence (EFI) [28] algorithm to eliminate engineering bias from the results of the study. Both the good and bad training DOF sets used thirty DOFs at ten triaxial response locations and the validation DOF set used twelve DOFs at four triaxial response locations. Note that the same validation DOF set was used regardless of the training DOF set. The good DOF set was selected with the typical EFI process and metric for triaxial accelerometers, the selected (good) locations are shown in Figure 4. The bad DOF set also used the typical EFI process for triaxial accelerometers, but the EFI metric was inverted so the worst sensor locations were chosen, the selected (bad) locations are shown in Figure 5. The validation DOF set was also selected with the standard EFI process and metric (for triaxial accelerometers), but the algorithm was initialized with the good and bad DOF sets, the selected (validation) locations are shown in Figure 6.

The “truth” target responses for the overfitting study were computed by applying broadband random excitation to triaxial input DOFs at the corners of the frame (twelve DOFs total) in the truth model. The input DOFs are shown in Figure 7.

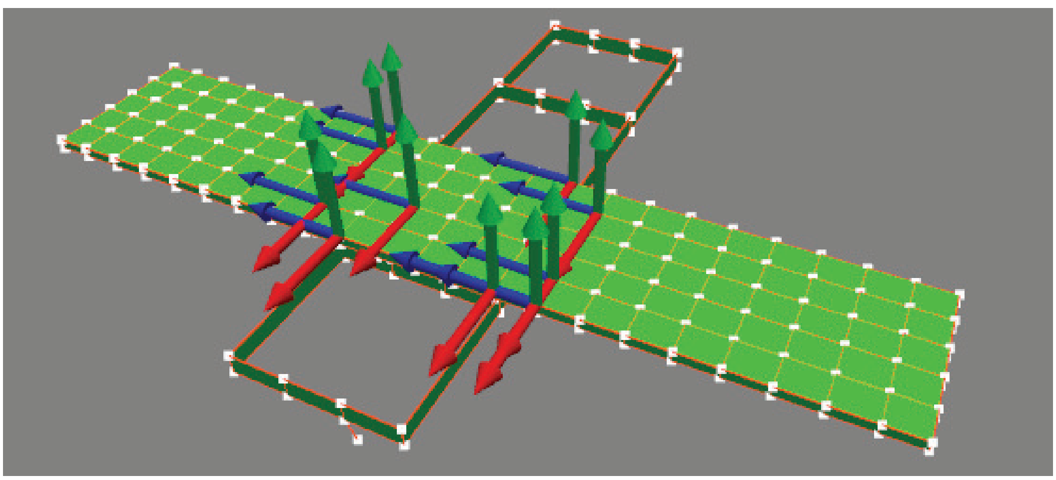

Fig. 4 The good set of response DOFs for the overfitting study.

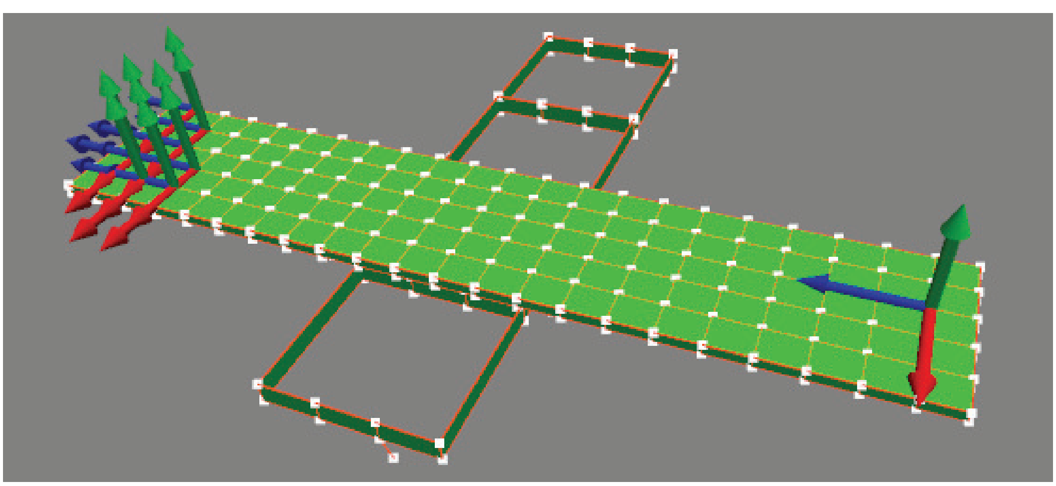

Fig. 5 The bad set of response DOFs for the overfitting study.

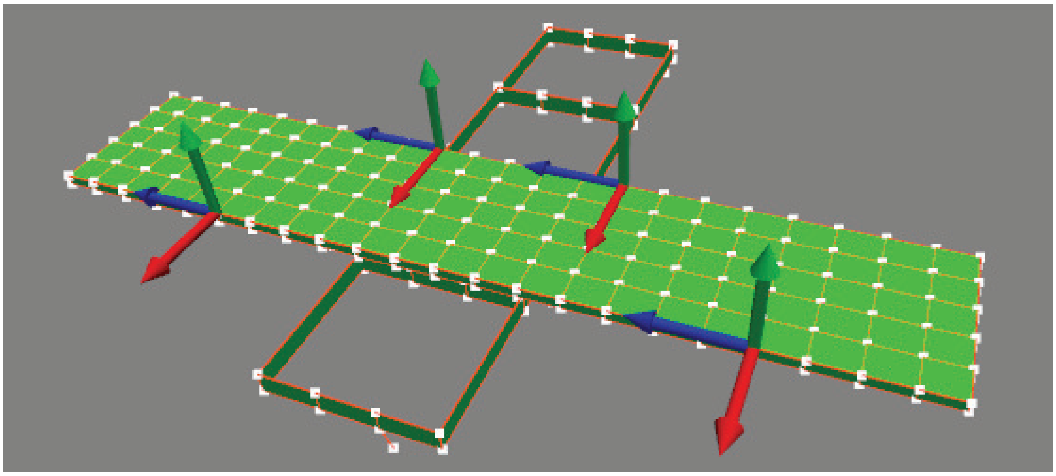

Fig. 6 The validation set of response DOFs for the overfitting study.

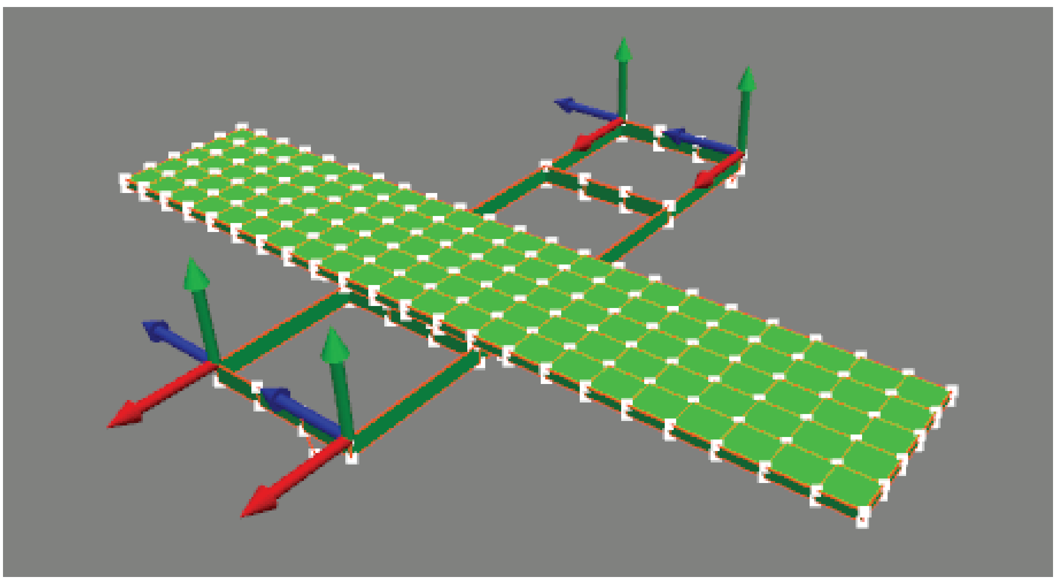

Fig. 7 The input DOFs for the overfitting study.

The spectral responses and inputs were computed as phase referenced spectra, using a force DOF as the reference and the signal processing parameters that are shown in Table 1. The responses with errors, which will be referred to as the "noised responses", were computed by adding broadband random noise to the truth response spectra, prior to phase referencing and averaging. Note that the signal-to-noise ratio (SNR) for the noised responses was tuned so an ISE with modeling errors or response errors would result in similar levels of overfitting, as determined by the amplitude errors in the estimated sources, while still having a typical SNR for vibration measurements. The DOF averaged SNR and summed (truth and noised) response power spectral density (PSD) for all the response DOFs in the overfitting study are shown in Figure 8. This plot shows that the noised response has a good signal to noise ratio and that the noise is not dramatically contaminating the truth responses.

The models and synthesized response data for the overfitting study were combined three different ways to match the different types of error that could contaminate an ISE problem. All the model/data combinations were used with both the good and bad training response DOFs, depending on the hypothesis that was being tested, and will be referred to accordingly. The model combinations were:

1. The truth model and truth response data were combined to create the baseline ISE problem
2. The truth model and noised response data were combined to create the response error ISE problem
3. The test model and truth response data were combined to create the modeling error ISE problem

Table 1 Signal processing parameters for spectra computation.

Parameter	Setting
Sampling Frequency	4,000 Hz
Frequency Resolution	1 Hz
Number of Averages	100
Window Type	Hanning

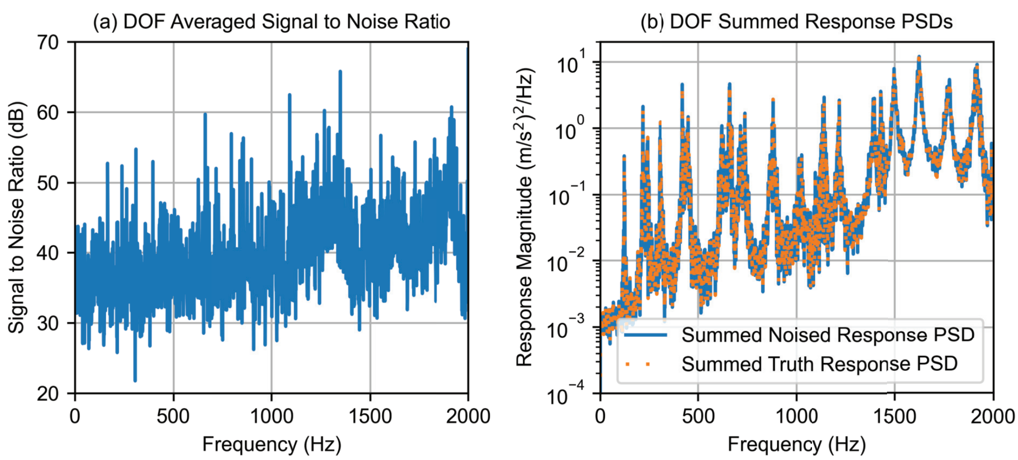

Fig. 8 DOF averaged signal to noise ratio for summed (truth and noised) response for all the response DOFs in the overfitting study.

The objective of the ISE problem in this example was to recover the "truth" sources that were used to compute truth responses at the input DOFs that are shown in Figure 7. Since the truth sources are known in this case, a comparison between the summed truth and estimated source PSDs can be used as a simple metric to show how significant the overfitting is for the different model/data combinations. The comparison between the truth and estimated source PSDs for both the good and bad training DOF sets is shown in Figure 9 for the baseline ISE problem, Figure 10 for the response error ISE problem, and Figure 11 for the modeling error ISE problem. These plots show that either training set can accurately recover the sources when there are not response or modeling errors in the ISE problem, but that there are significant errors when

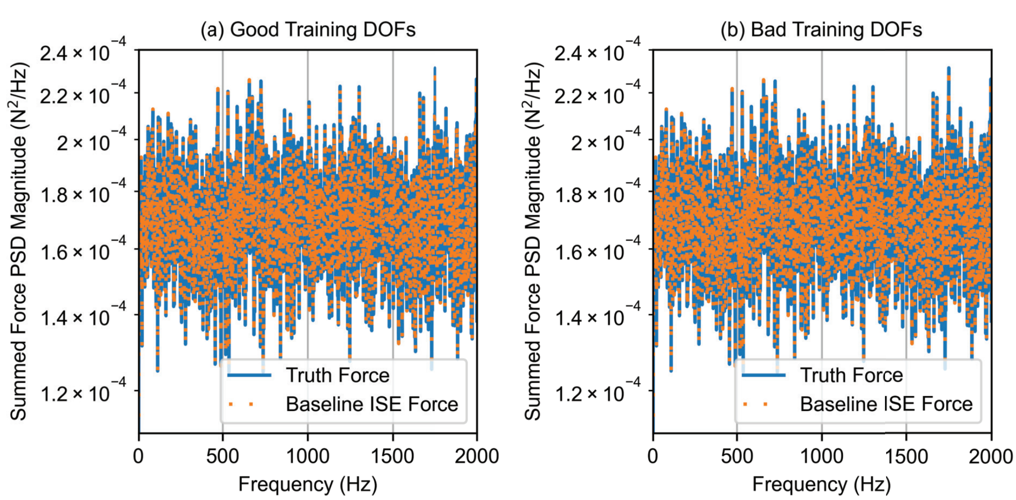

Fig. 9 Summed truth and estimated source PSDs for the baseline ISE problem for the different training DOF sets.

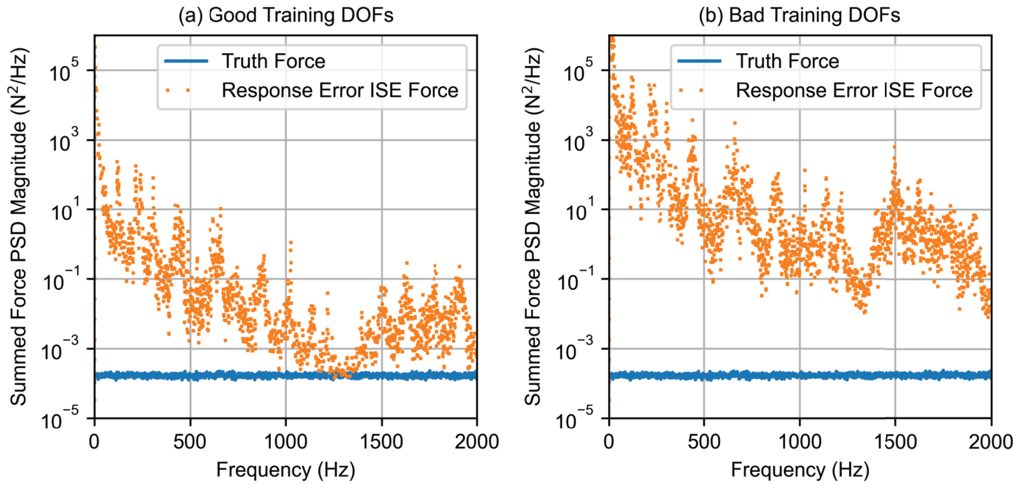

Fig. 10 Summed truth and estimated source PSDs for the response error ISE problem for the different training DOF sets.

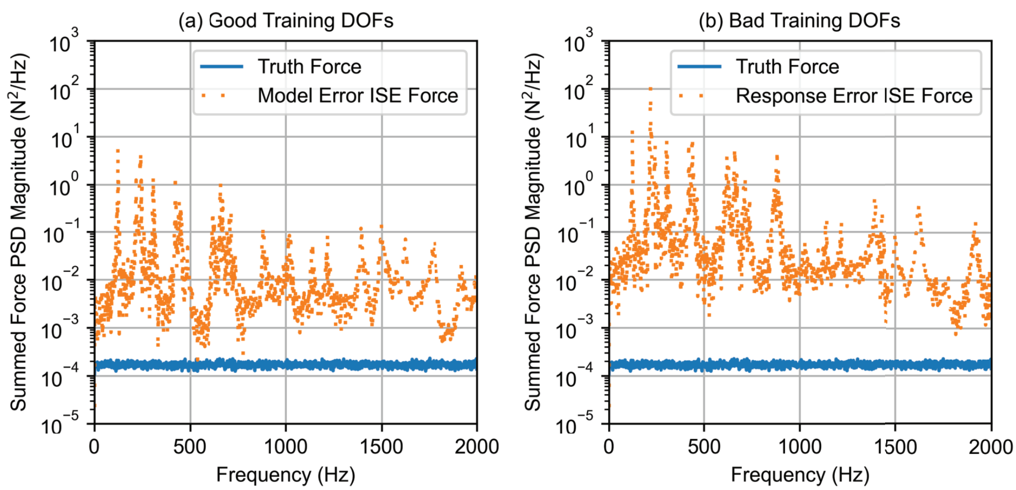

Fig. 11 Summed truth and estimated source PSDs for the modeling error ISE problem for the different training DOF sets.

there are response or modeling errors. Further, these plots show that the bad training DOFs result in worse source estimation errors than the good training DOFs (as expected). Lastly, the overfitting is slightly more significant when there are response errors compared to modeling errors. However, the reason for this increased sensitivity is unclear and was not explored in this work.

Testing The Hypothesis For Overfitting

The hypothesis for the root cause of overfitting was tested by comparing the singular responses (computed with the transformed response that is shown in (11)) from the ISE problems with response and modeling errors to the singular responses from the baseline ISE problem, which represents the truth singular responses. These comparisons can be seen in Figure 12 and Figure 13 for the ISE problem with response and modeling errors, respectively. The same comparisons were made for the singular responses that were not scaled by the inverted singular values (by removing $[S]^{\dagger}$ from the equation), as shown in Figure 14 and Figure 15 for the ISE problem with response and modeling errors, respectively. Note that these comparisons were made with the singular responses that were computed with the good training DOFs only.

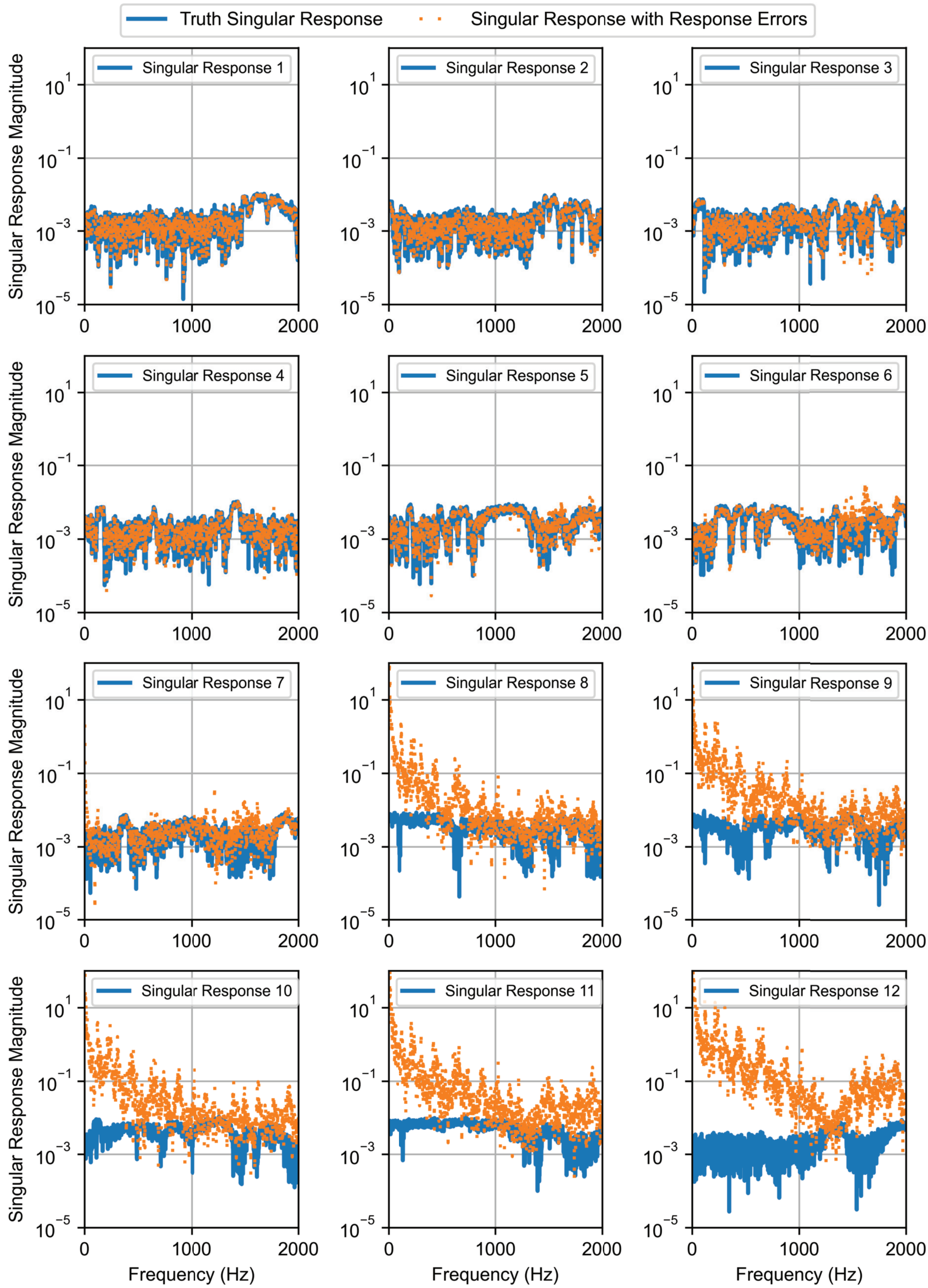

Fig. 12 The singular responses (scaled the inverted singular values) for the response error and baseline ISE problems.

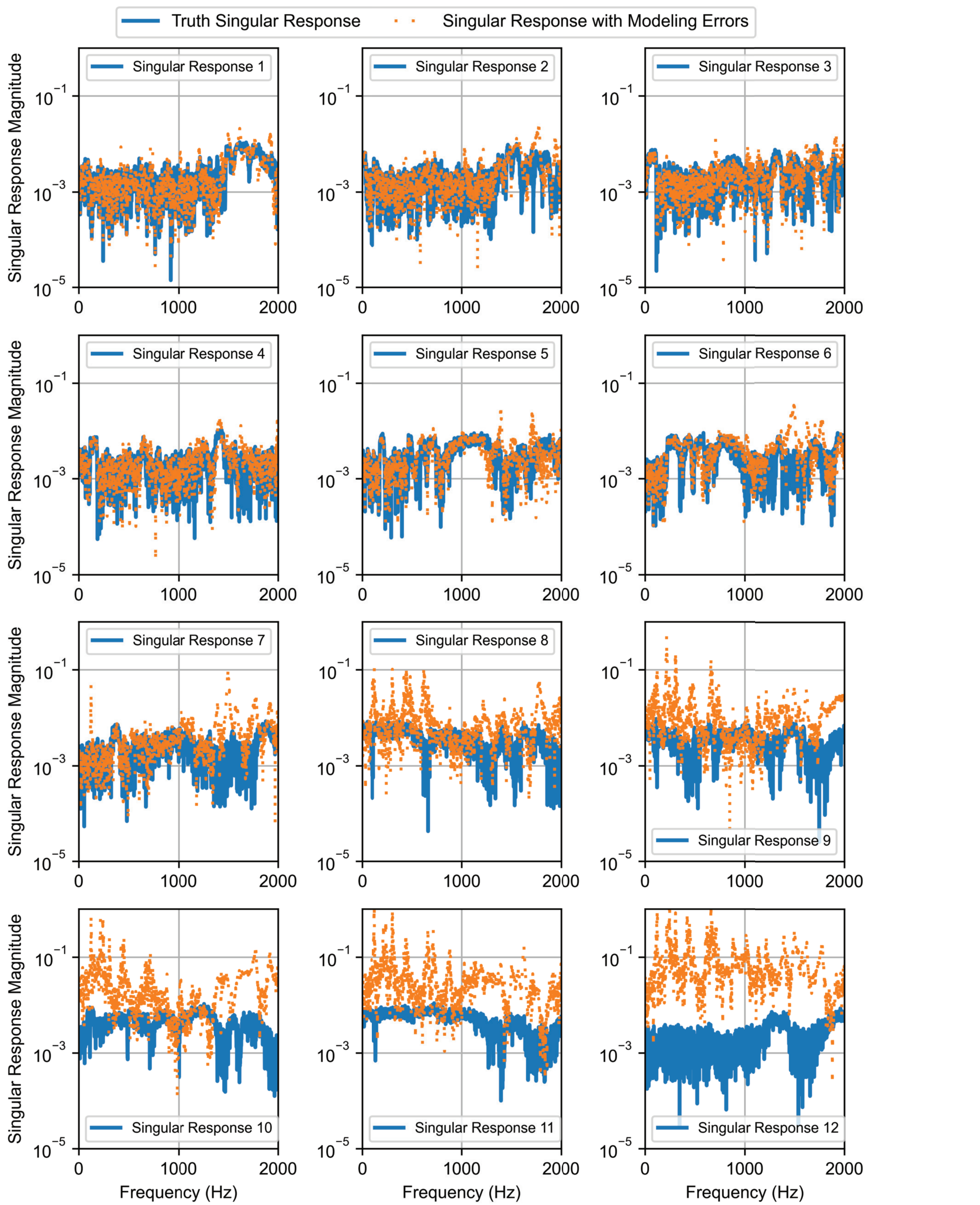

Fig. 13 The singular responses (scaled the inverted singular values) for the modeling error and baseline ISE problems.

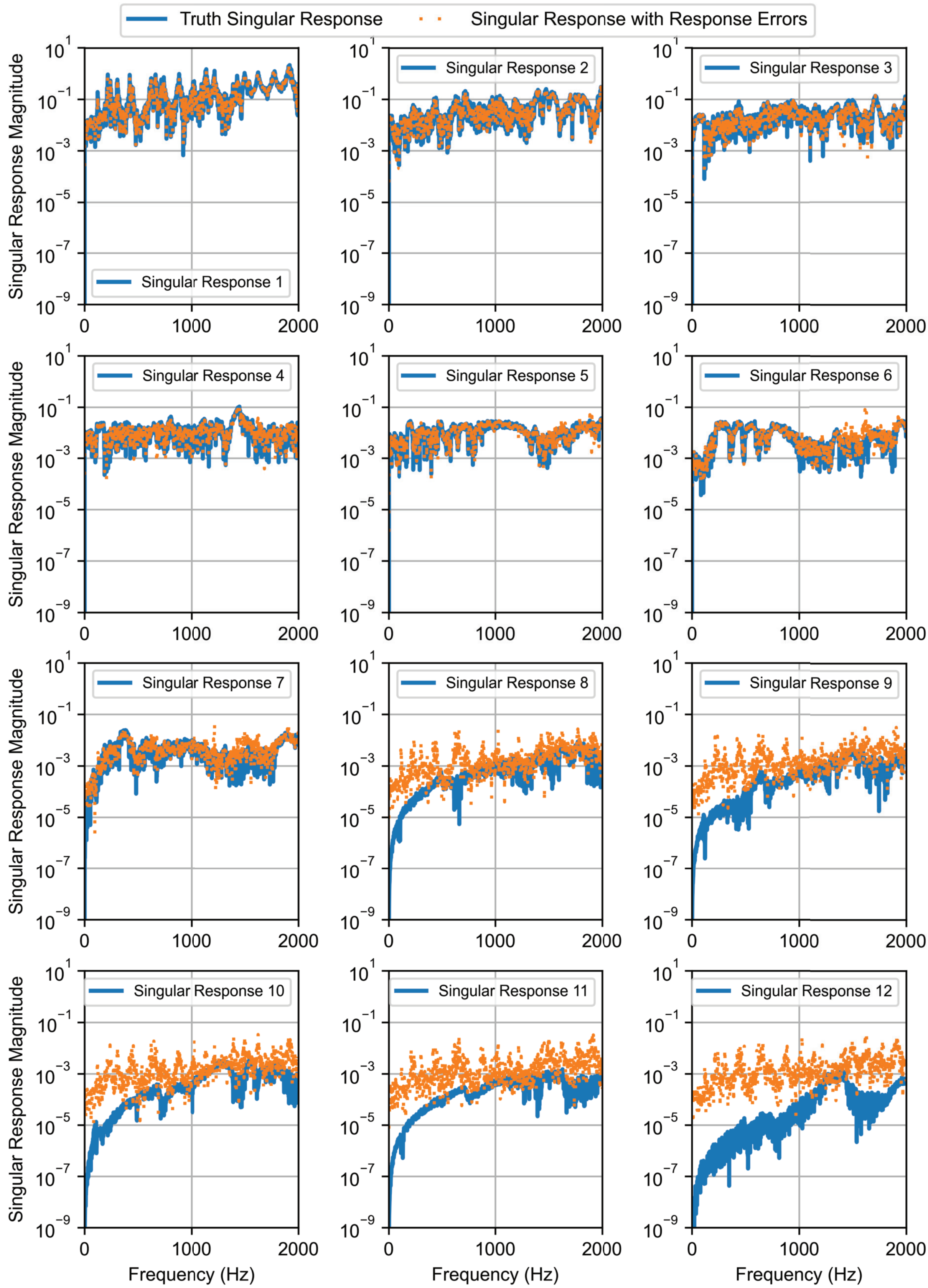

Fig. 14 The singular responses (not scaled by the inverted singular values) for the response error and baseline ISE problems.

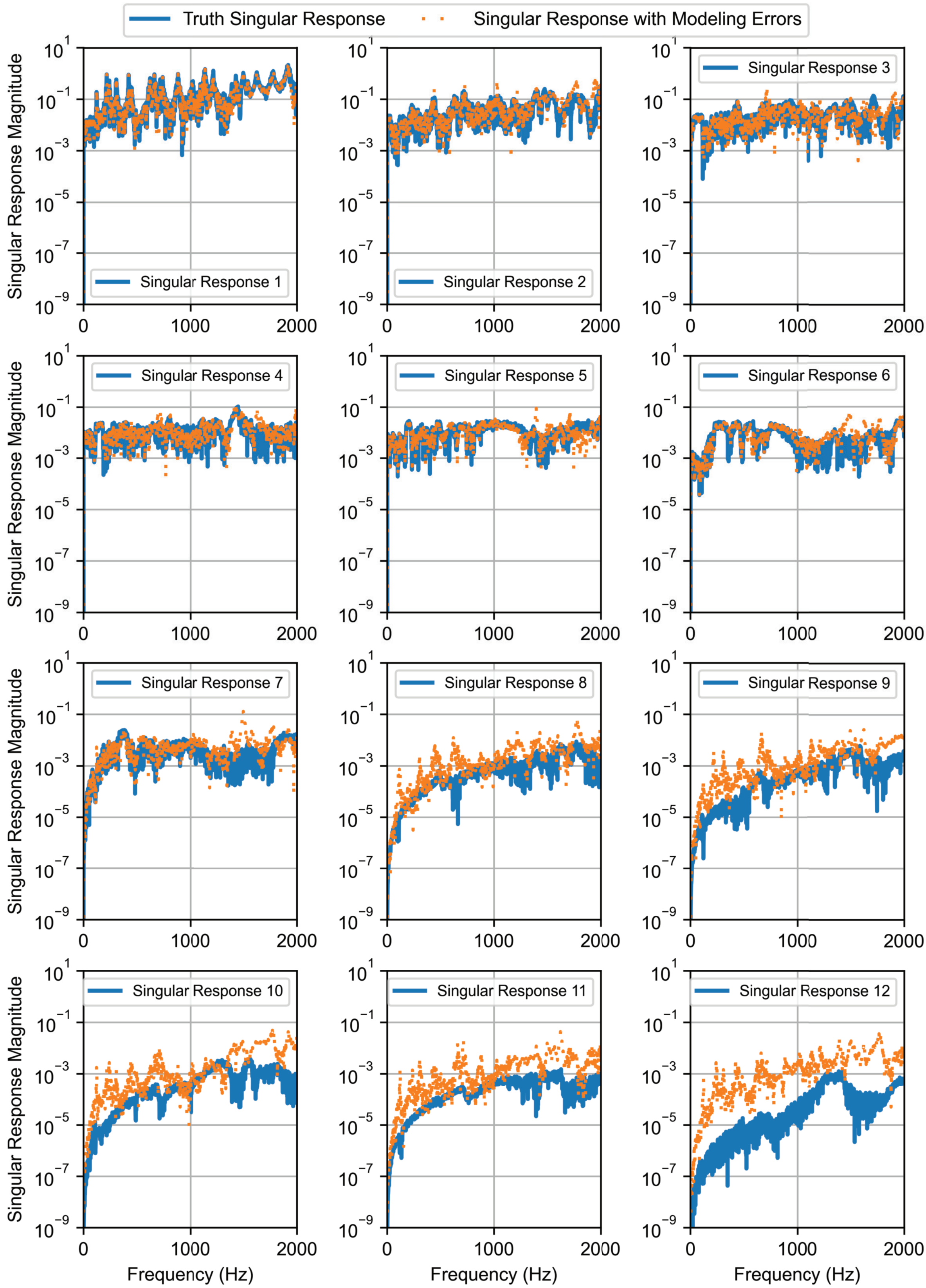

Fig. 15 The singular responses (not scaled by the inverted singular values) for the modeling error and baseline ISE problems.

The singular responses are significantly overpredicted for both the response and modeling error ISE problems, regardless of if singular responses scaled by the inverted singular value. However, it can clearly be seen that scaling the singular responses by the inverted singular values increases the significance of the singular response errors, given on the relative amplitude of the errors compared to the amplitude of the truth singular responses. These comparisons seem to confirm the hypothesis that overfitting is caused by transformation errors when the responses are projected onto the left singular vectors of the FRF matrix, and that the significance of the overfitting is controlled by the relative amplitudes of the singular values of the FRF matrix (i.e., the condition number). Interestingly, the singular response errors seem to result in the same spectrum shape as the errors in the sources that were shown Figure 10 and Figure 11, providing further evidence that the transformation errors are likely the primary cause of overfitting in ISE.

The most significant singular response errors are seen in the singular responses that are associated with the small singular values (9-12 in this case) for both the response and modeling error ISE cases. This finding seems confirm the assumption for how the TSVD and Tikhonov regularization mitigate overfitting. However, it is interesting to note that moderate singular response errors are seen in the singular responses that are associated with the large singular values, when there are modeling errors in the ISE problem. But not when there are response errors. This makes intuitive sense because the modeling errors will likely contaminate all the singular vectors of the FRF matrix, since there are fundamental errors in the mode shapes that are described by the FRFs. On the other hand, the response errors in this example contaminated the response deflection shapes with random noise, which likely can't be fit by simplistic deflection shapes in the FRFs. As such, the response errors likely map to the complicated singular vectors in the FRF matrix, which are associated with the small singular values.

Evaluating How Regularization Mitigates Overfitting

The Tikhonov regularized singular responses, as formulated in (15), were computed to demonstrate how regularization can be used to mitigate overfitting. In this case, the regularization parameter was automatically selected using the L-curve method (on a frequency line by frequency line basis) that is described in [9, 29]. Note that only the good training DOFs were used here, for brevity. The regularized source estimates were compared to the truth sources to evaluate how well the regularization resolved the overfitting issue as shown in Figure 16 and Figure 17 for the response and modeling error ISE problems, respectively. The regularization dramatically reduces the overfitting issue and actually underestimates the sources. It is unclear if further tuning could increase accuracy of the source estimation, especially if the truth forces are unknown. Regardless, this example seemed sufficient to demonstrate the effects of regularization and further tuning was not attempted since it was outside the scope of this work.

The comparisons between the truth and regularized singular responses (scaled by the inverted singular values) are shown in Figure 18 for the response error ISE problem and Figure 19 for the modeling error ISE problem. These comparisons clearly demonstrate that Tikhonov regularization is mitigating the errors in the singular responses that are associated with the small singular values, as expected. It is interesting to note that while the singular responses are generally underpredicted,

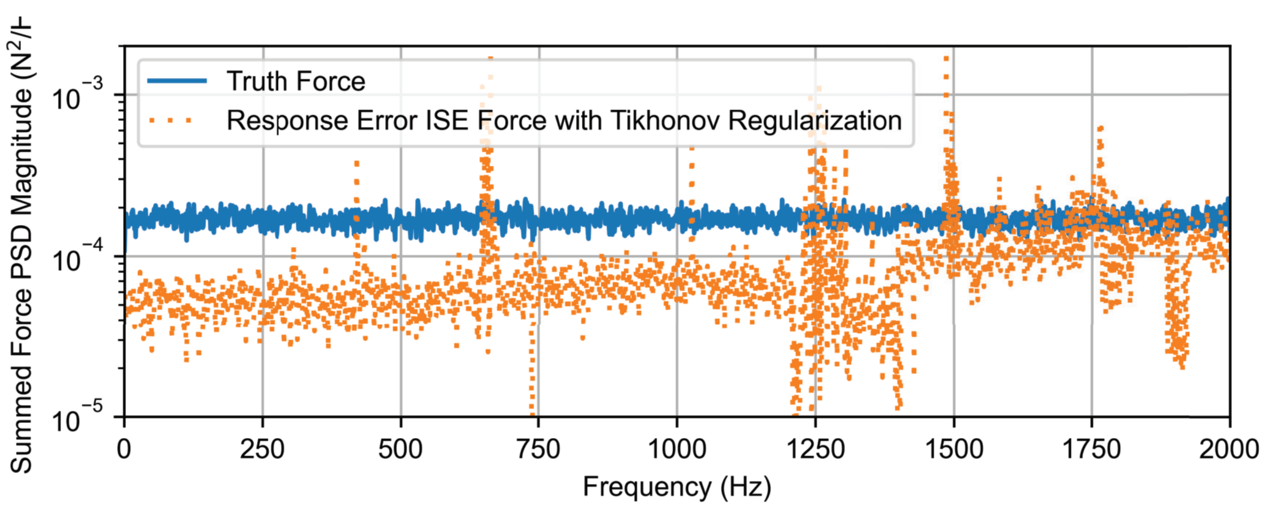

Fig. 16 Summed truth and estimated source PSDs for the response error ISE problem with the good training DOFs.

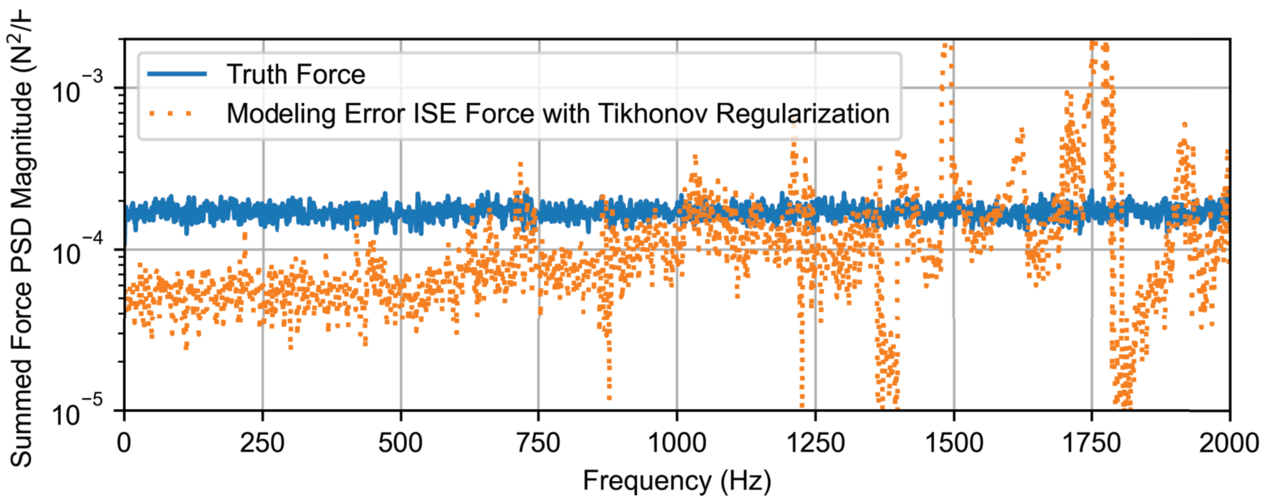

Fig. 17 Summed truth and estimated source PSDs for the modeling error ISE problem with the good training DOFs.

the errors in the singular responses do not seem to have a similar spectrum shape to the errors that are seen in the estimated sources, which contradicts the finding from the overfit case that was shown in Figure 12 and Figure 13. However, it is unclear what (if anything) this contradiction means for the hypothesis on the cause of overfitting, given the extreme flexibility in selecting the regularization parameter.

Testing the CV Hypothesis

The efficacy of CV checks was evaluated using the different DOF sets that were described above. First, the sources were estimated with both the good and bad training DOFs and then the estimated sources were then used to reconstruct the responses at the training and validation DOFs. The reconstructed responses (for both the training and validation DOFs) were compared to the target responses to see if the responses at either the training or validation DOFs could predict overfitting. For brevity, the average dB error for all the DOFs in either the training or validation sets was used as metric for the error in the reconstructed responses. The formula for this error metric is shown in (16), where $\{X\}$ is a vector of response PSDs for either the reconstructed or target responses, depending on the superscript, and n is the number of response DOFs in the given set.

$$\varepsilon^{reconstructed} = 10 * \log_{10}\left(\frac{\sum\left(\{X^{reconstructed}\} - \{X^{target}\}\right)}{n}\right) \tag{16}$$

The reconstructed response error for the training and validation DOFs when the sources are estimated with both the good and bad training DOFs is shown in Figure 20 and Figure 21 for the ISE problems with response and modeling errors, respectively. Both these plots show that the validation and training DOFs show similar levels of reconstructed response error when the good training DOFs are used to estimate the sources. Conversely, the validation DOFs show significantly higher reconstructed response error than training DOFs when the bad training DOFs are used to estimate the sources. This seems to confirm the previously described hypothesis that CV checks may be insensitive to overfitting errors if the training DOFs describe the response deflection shapes well, but further work should be done to see if this is a general finding.

It should be noted that the CV check seems to be more sensitive to the overfitting error when there are responses errors in the ISE problem vs. when there are modeling errors in the ISE problem. This could be due to the fact that the responses errors were essentially random perturbations of the response deflection shapes, which could accentuate the differences in the deflection shapes that are described by the training and validation DOFs (increasing the sensitivity of the CV check). However, the increased sensitivity in the CV check could simply be due to the fact that the overfitting is much worse in the response error ISE problem with the bad training DOFs than the modeling error ISE problem with the bad training DOFs, as evidenced source estimation errors in Figure 10 and Figure 11. As such, further study should be done to understand how CV checks apply to overfitting.

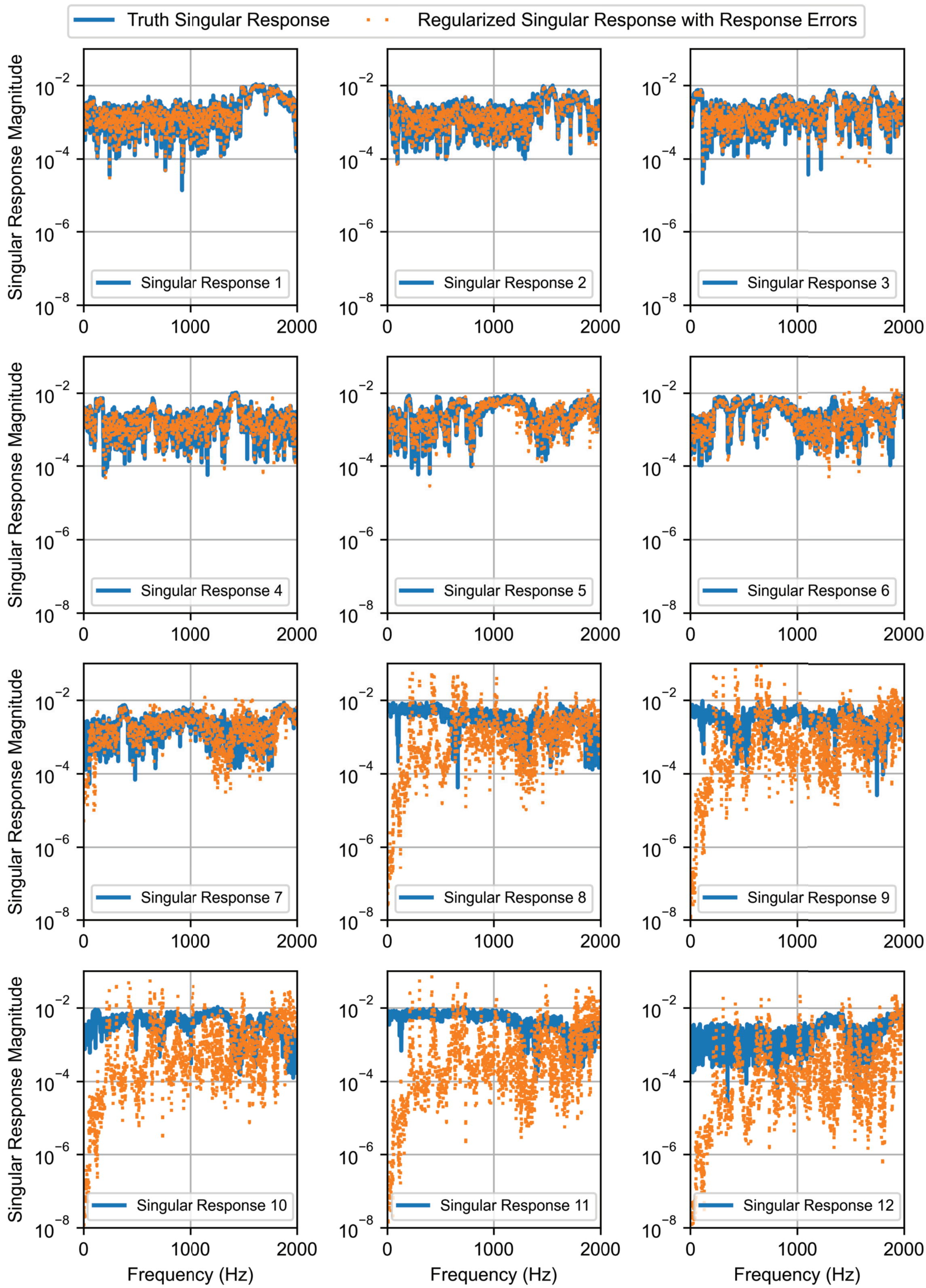

Fig. 18 Regularized singular responses for the response error ISE problem compared to the unregularized baseline ISE problem.

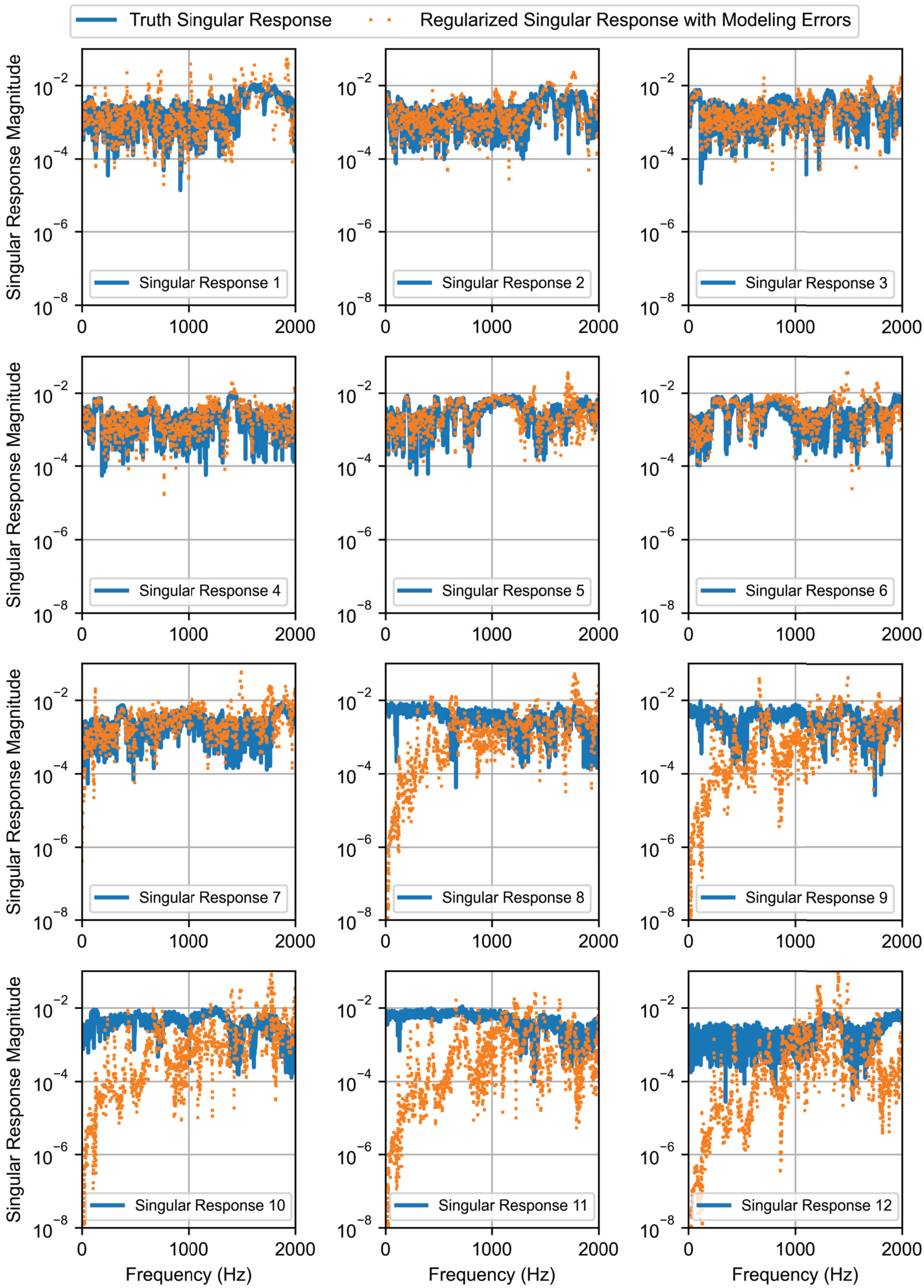

Fig. 19 Regularized singular responses for the modeling error ISE problem compared to the unregularized baseline ISE problem.

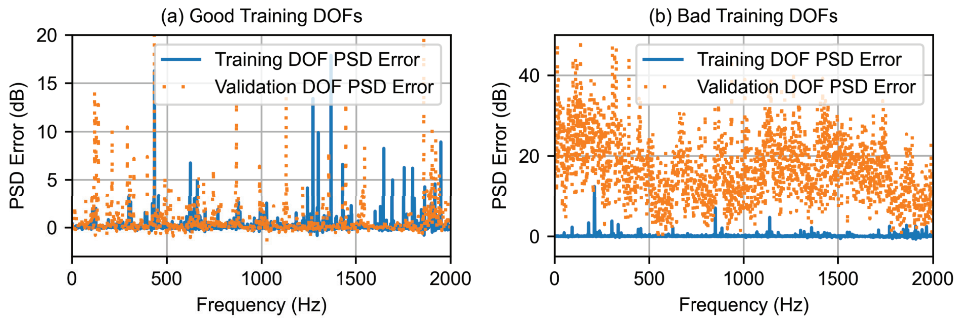

Fig. 20 Reconstructed response error for the training and validation DOFs in the response error ISE problem from sources that were estimated with both the good and bad training DOFs.

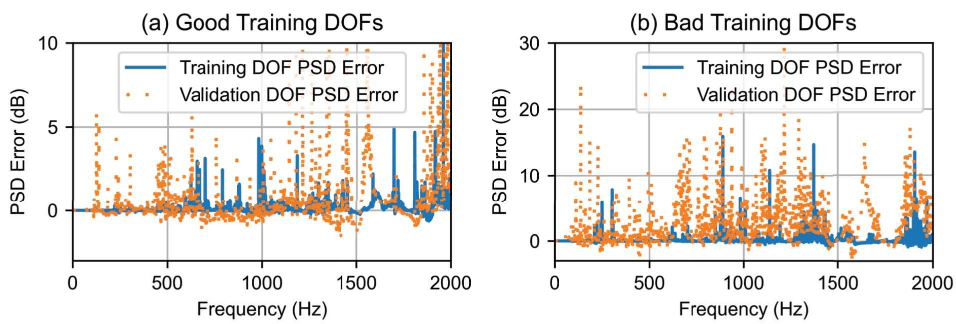

Fig. 21 Reconstructed response error for the training and validation DOFs in the modeling error ISE problem from sources that were estimated with both the good and bad training DOFs.

Conclusion

This paper developed a theoretical understanding for overfitting in ISE, which led to a hypothesis that overfitting is fundamentally caused by transformation errors when the target response is projected onto the left singular vectors of the FRF matrix, where the relative amplitudes of the singular values (i.e., the condition number) determine the significance of the overfitting problem. This hypothesis was tested and seemingly confirmed on two different ISE problems, where there were errors in the target responses and errors in the FRFs. The overfitting hypothesis was also applied to regularization and CV checks to better understand how those methods can be used to mitigate and identify overfitting errors. It was shown that CV checks may be insensitive to overfitting if high quality response DOFs are used in the training set for the ISE, since the validation set may not add any information to the ISE problem.

The concepts in this paper were described in a qualitative manner and future work should attempt to describe overfitting in a mathematically rigorous fashion. Future work should also include the development of a framework for overfitting in ISE problems so the different error, mitigation methods, and data analysis methods can be discussed using common terminology. Further work should also be done to understand the efficacy of CV checks in ISE so better methods for identifying overfitting errors can be developed. Lastly, work should be done to see if other ISE techniques, such as the sum of weighted acceleration technique (SWAT) or Kalman filtering, that don't rely on FRF matrix inversion have a similar root cause for overfitting.

Acknowledgments *This article has been authored by an employee of National Technology & Engineering Solutions of Sandia, LLC under Contract No. DE-NA0003525 with the U.S. Department of Energy (DOE). The employee owns all right, title and interest in and to the article and is solely responsible for its contents. The United States Government retains and the publisher, by accepting the article for publication, acknowledges that the United States Government retains a non-exclusive, paid-up, irrevocable, world-wide license to publish or reproduce the published form of this article or allow others to do so, for United States Government purposes. The DOE will provide public access to these results of federally sponsored research in accordance with the DOE Public Access Plan* https://www.energy.gov/downloads/doe-public-access-plan. *This paper describes objective technical results and analysis. Any subjective views or opinions that might be expressed in the paper do not necessarily represent the views of the U.S. Department of Energy or the United States Government.*

References

1. J. Sanchez and H. Benaroya, “Review of force reconstruction techniques,” Journal of Sound and Vibration, vol. 333, no. 14, pp. 2999–3018, 2014/07/07/ 2014, doi:https://doi.org/10.1016/j.jsv.2014.02.025.
2. M. V. van der Seijs, D. de Klerk, and D. J. Rixen, “General framework for transfer path analysis: History, theory and classification of techniques,” Mechanical Systems and Signal Processing, vol. 68-69, pp. 217–244, 2016/02/01/2016, doi:https://doi.org/10.1016/j.ymssp.2015.08.004.
3. P. Daborn, “Smarter dynamic testing of critical structures,” PhD dissertation, Aerospace Department, University of Bristol, 2014.
4. S. Carter and B. Owens, “Errors using six degree-of-freedom force estimates to translate environments system-to- system,” in ISMA, Leuven, BE, 2022.
5. S. Carter and B. Owens, “Using Component Based TPA to Translate Vibration Environments Between Versions of the Round Robin Structure with FRFs Derived from Analytical Models,” in Proceedings of IMAC XLI, the 41st International Modal Analysis Conference, Austin, 2023.
6. A. N. Thite and D. J. Thompson, “The quantification of structure-borne transmission paths by inverse methods. Part 1: Improved singular value rejection methods,” Journal of Sound and Vibration, vol. 264, no. 2, pp. 411–431, 2003/07/03/ 2003, doi:https://doi.org/10.1016/S0022-460X(02)01202-6.
7. A. N. Thite and D. J. Thompson, “The quantification of structure-borne transmission paths by inverse methods. Part 2: Use of regularization techniques,” Journal of Sound and Vibration, vol. 264, no. 2, pp. 433–451, 2003/07/03/2003, doi:https://doi.org/10.1016/S0022-460X(02)01203-8.
8. R. Schultz, “A Demonstration of Force Estimation and Regularization Methods for Multi-Shaker Testing,” 2020, pp. 229-243.
9. S. Carter, “Thoughts on Using Sparse Inverse Solutions in Transfer Path Analysis,” in Proceedings of IMAC XLII, the 42nd International Modal Analysis Conference, Orlando, 2024.
10. M. Van der Seijs, D. van den Bosch, D. Rixen, and D. Klerk, “An improved methodology for the virtual point transformation of measured frequency response functions in dynamic substructuring,” in Proceedings of the 4th International Conference on Computational Methods in Structural Dynamics and Earthquake Engineering, Kos Island, 2013, pp. 4334–4347, doi:10.7712/120113.4816.C1539.
11. R. Schultz and P. Avitabile, “Shape-constrained Input Estimation for Efficient Multi-shaker Vibration Testing,” Experimental Techniques, vol. 44, no. 4, pp. 409-423, 2020/08/01 2020, doi:10.1007/s40799-020-00361-0.
12. D. Ocepek, F. Trainotti, G. Cepon, M. Boltezar, and D. J. Rixen, “Different displacement reduction spaces for the use in admittance-based TPA methods,” in Proceedings of IMAC XLII, the 42nd International Modal Analysis Conference, Orlando, 2024.
13. A. N. Thite and D. J. Thompson, “Selection of response measurement locations to improve inverse force determination,” Applied Acoustics, vol. 67, no. 8, pp. 797–818, 2006/08/01/ 2006, doi:https://doi.org/10.1016/j.apacoust.2006.01.001.
14. C. Beale, R. Schultz, C. Smith, and T. Walsh, “Degree of Freedom Selection Approaches for MIMO Vibration Test Design,” in Proceedings of IMAC-XL, the 40th International Modal Analysis Conference, Orlando, 2022, doi:10.1007/978-3-031-05405-1_10.
15. J. DeClerck, “Inverse Force Estimation for TPA,” 2000.
16. M. Haeussler and D. Rixen, “Optimal transformation of frequency response functions on interface deformation modes,” in Proceedings of IMAC XXXV, the 35th International Modal Analysis Conference, Los Angeles 2017.
17. F. Trainotti, T. Bregar, S. W. B. Klaassen, and D. J. Rixen, “Experimental decoupling of substructures by singular vector transformation,” Mechanical Systems and Signal Processing, vol. 163, p. 108092, 2022/01/15/ 2022, doi:https://doi.org/10.1016/j.ymssp.2021.108092.
18. D. Rohe, R. Schultz, and N. Hunter, “Rattlesnake User’s Manual,” Sandia National Laboratories, 2021.
19. L. Meirovitch and H. Baruh, “The implementation of modal filters for control of structures,” Journal of Guidance Control and Dynamics, vol. 8, pp. 707–716, 1985.
20. D. Otte, “Development and evaluation of singular value analysis methodologies for studying multivariate noise and vibration problems,” Department of Mechanical Engineering, Katholieke Universiteit Leuven, 1994.
21. T. Schoenherr, “Using Modal Projection Error to Optimize Accelerometer Locations for a Modal Filter,” in Proceedings of IMAC XLII, the 42nd International Modal Analysis Conference, Orlando, 2024.
22. T. Hastie, R. Tibshirani, and J. Friedman, The Elements of Statistical Learning: Data Mining, Inference, and Prediction, 2nd Edition ed. New York: Springer New York, 2017.
23. M. Aucejo and O. De Smet, “Bayesian source identification using local priors,” Mechanical Systems and Signal Processing, vol. 66-67, pp. 120–136, 2016/01/01/ 2016, doi:https://doi.org/10.1016/j.ymssp.2015.05.004.
24. M. Aucejo and O. De Smet, “An optimal Bayesian regularization for force reconstruction problems,” Mechanical Systems and Signal Processing, vol. 126, pp. 98–115, 2019/07/01/ 2019, doi:https://doi.org/10.1016/j.ymssp.2019.02.021.
25. T. Hastie, R. Tibshirani, and M. Wainwright, Statistical Learning with Sparsity: The Lasso and Generalizations (Monographs on Statistics and Applied Probability 143). Boca Raton, FL: Chapman & Hall/CRC, 2015.
26. D. Roettgen and A. Linderholt, “Substructuring excercises on combinations of steel and aluminum components of the benchmark structure of the technical division on dynamic substructures,” in The 40th International Modal Analysis Conference, Orlando, 2022.
27. D. Roettgen, G. Lopp, A. Jaramillo, and B. Moldenhauer, “Experimental Substructuring of the Dynamic Substructures Round-Robin Testbed,” 2022, pp. 119-123.
28. D. Kammer and M. Tinker, “Optimal placement of triaxial accelerometers for modal vibration tests,” Mechanical Systems and Signal Processing, vol. 18, pp. 29–41, 01/31 2004, doi:10.1016/S0888-3270(03)00017-7.
29. H. G. Choi, A. N. Thite, and D. J. Thompson, “Comparison of methods for parameter selection in Tikhonov regularization with application to inverse force determination,” Journal of Sound and Vibration, vol. 304, no. 3, pp. 894–917, 2007/07/24/ 2007, doi:https://doi.org/10.1016/j.jsv.2007.03.040.